A NOVEL RUMINANT EMISSION MEASUREMENT SYSTEM: PART I. DESIGN EVALUATION AND DESCRIPTION

G. D. N. Maia, B. C. Ramirez, A. R. Green, L. F. Rodriguez,
J. R. Segers, D. W. Shike, R. S. Gates

ABSTRACT. *Methane (CH_4) generated by cattle is both a major source of greenhouse gas emissions and a powerful indicator of feed conversion efficiency; thus, accurate quantification of CH_4 production is required for addressing future global food security without neglecting environmental impacts. A newly developed Ruminant Emission Measurement System (REMS) supports research on the relationships between bovine nutrition, genetics, and management strategies by measuring eructated CH_4 emissions from ruminal activity. REMS is a substantial improvement and extension of the chamber technique, which is considered the standard method to quantify ruminant CH_4 generation. Part I of this two-part series describes the design and evaluation of REMS. An uncertainty analysis of chamber emission rate (ER) was conducted to identify critical measurement component contributions to overall ER uncertainty and guide component selection. In Part II, REMS commissioning was performed and a method for system validation including overall emission uncertainty is reported. REMS consists of six positive pressure ventilated hood-type chambers individually equipped with a thermal environmental control subsystem, fresh air supply control subsystem, and gas sampling subsystem. Estimates of the standard uncertainty for each measurement parameter were quantified and propagated through the ER equation derived from CH_4 and air mass flow balances. A sensitivity analysis was conducted to assess the contribution of each parameter to the emission rate standard uncertainty (absolute = ΔER; relative = $\%\Delta ER$) under predicted normal operation by varying gas analyzer and ventilation measurement uncertainties as anticipated with REMS use. Results showed that expanded $\%\Delta ER$ (~95% confidence level) associated with the methane ER computation was approximately 5.9% for ER values between 3.5 and 17.2 g h^{-1}. Ventilation rate and gas concentration measurements were the major sources of uncertainty, contributing about 69% and 29%, respectively, to the uncertainty associated with methane ER values. This work provides the foundation for future studies using respiration chambers to include a stated standard uncertainty associated with animal emission measurements.*

Keywords. *Climate change, Feeding, Food security, Methane production, Uncertainty.*

In 2011, the agricultural sector contributed approximately 8.1% of total greenhouse gas emissions in the U.S. (EPA, 2013). Methane (CH_4) produced from enteric fermentation, primarily from beef and dairy cattle, was estimated to account for 23.4% of total CH_4 emissions in the U.S. (EPA, 2013). Accurate CH_4 emissions quantification has serious implications for ruminant livestock production, food security, and the environment (Schmidhuber and Tubiello, 2007; Skoet and Stamoulis, 2006). It is also a critical requirement for evaluating possible mitigation strategies (Makkar and Vercoe, 2007; McGinn, 2006). Process-based CH_4 emission evaluations (Tier 3 methods) using a variety of diets can substantially increase the quality of inventories used to estimate CH_4 global emissions by providing new variables and information that will affect emission factor estimates currently used in Tier 1 and 2 methods (IPCC, 2006).

Methane is a key parameter in evaluating ruminant production efficiency (McGinn, 2006). As global demand increases for enhanced animal production efficiency without adverse environment effects, there is an urgent need to maximize ruminant feed conversion efficiency while accurately quantifying and understanding CH_4 emissions. Cattle enteric and rumen CH_4 production is a result of anaerobic microbial fermentation of hydrolyzed dietary carbohydrates, representing a loss of between 2% and 12% of the gross metabolic energy intake of the animal (Johnson and Johnson, 1995).

The "gold standard" method for animal energetics and metabolism research has been the open-circuit indirect calorimeter and respiration chamber (Bhatta et al., 2007;

Submitted for review in April 2014 as manuscript number PAFS 10752; approved for publication by the Plant, Animal, & Facility Systems Community of ASABE in May 2015.

The authors are **Guilherme D. N. Maia, ASABE Member,** Post-Doctoral Research Associate, Department of Agricultural and Biological Engineering, University of Illinois at Urbana-Champaign, Urbana, Illinois; **Brett C. Ramirez, ASABE Member,** Graduate Research Assistant, Department of Agricultural and Biosystems Engineering, Iowa State University, Ames, Iowa; **Angela R. Green,** Assistant Professor, and **Luis F. Rodríguez,** Associate Professor, Department of Agricultural and Biological Engineering, University of Illinois Urbana-Champaign, Urbana, Illinois; **Jacob R. Segers,** Assistant Professor, Department of Animal and Dairy Sciences, University of Georgia, Athens, Georgia; **Daniel W. Shike,** Assistant Professor, Department of Animal Sciences, and **Richard S. Gates, ASABE Fellow,** Professor, Department of Agricultural and Biological Engineering, University of Illinois Urbana-Champaign, Urbana, Illinois. **Corresponding author:** Guilherme Maia, AESB MC-644, 1304 W. Pennsylvania Ave., Urbana, IL 61801; phone: 859-608-7570; e-mail: gdnmaia@gmail.com.

Vol. 58(3): 749-762 ISSN 2151-0032 DOI 10.13031/trans.58.10752

Storm et al., 2012). Chamber techniques measure respiratory gas exchange, including CH_4 production from enteric fermentation, and have better accuracy and precision than alternative methods such as the sulfur hexafluoride (SF_6) tracer gas technique (Grainger et al., 2007; Muñoz et al., 2012; Pinares-Patiño et al., 2011). Mathematical models are necessary to assess national or global emissions, but accurate extrapolations are limited by accuracy and by the experimental data from which they are derived (Ellis et al., 2009; Gates et al., 2008; Storm et al., 2012). Micrometeorological methods for determining grazing animal emissions and CH_4 generation models of ruminal fermentation of feed and feed additives measured by the *in vitro* gas production technique provide reasonable accuracy compared to the chamber technique but are often difficult to validate and extrapolate (Bhatta et al., 2006; Murray et al., 1999; Tomkins et al., 2011). Although the chamber technique is considered the reference for ruminant CH_4 emissions measurements, a documented comprehensive error analysis is required for understanding the confidence in this technique (McGinn, 2006).

Few estimates of CH_4 emissions using the chamber technique have included a statement of uncertainty in published results (McGinn, 2006). For a computed quantity based on multiple measurements, such as animal emission rate (ER), there are many individual sources of errors, which are often unique to each monitoring system. Methods for instrument calibration combined with total system error evaluation have been documented for the chamber technique. For example, Nienaber and Maddy (1985) provided combined uncertainties ranging from 3.45% to 5.58% for an open-circuit indirect calorimeter system measuring heat production (in kilowatts). McGinn et al. (2004) reported 7% uncertainty for ER determined from the analysis of ventilation and gas concentration measurement sensitivities. Comprehensive uncertainty analyses are available for other applications, such as gravimetric sampling of particulate matter (Price and Lacey, 2003), and for other animal production systems, including ammonia emissions from field-scale broiler houses (Casey, 2005; Gates et al., 2009). Systematic documentation and an integrated methodology to assess system uncertainties are needed, especially in animal studies with the chamber technique.

Emission rate uncertainty is a critical design parameter; hence, it should be an integral part of the design analysis of any measurement system used in energetics or metabolism research. A detailed methodology with a worked example to quantify uncertainties associated with the chamber technique is provided here. The goal of this work is to introduce and describe a systematic approach to evaluate the Ruminant Emission Measurement System (REMS), which is an improvement and extension of the chamber technique. The design evaluation phase applies mathematical relationships and derivations to the system computations and measurements, which in turn guides subsystem development. In addition, this analysis estimates the ER absolute standard uncertainty (ΔER) and relative standard uncertainty ($\%\Delta ER = 100 \times ER/\Delta ER$) associated with ER determined by REMS. To achieve these goals, the objectives of this study were to:

- Document REMS design and key REMS subsystems, including characterizing and quantifying instrument standard uncertainties.
- Derive a REMS emission rate equation and its associated ER standard uncertainties.
- Perform a sensitivity analysis to assess measurement uncertainty contributions relative to ER standard uncertainties.

This analysis establishes a well-documented procedure to quantify methane ER uncertainty determined by REMS, and by extension, the instruments and operation of other respiration chambers and indirect calorimeters. This study precedes part II of this series, in which the system commissioning and performance using measured data were conducted to validate uncertainty estimates and assess potential systematic errors (Maia et al., 2015). Separation of the design evaluation and commissioning phases emphasizes the need to first use uncertainty analysis to guide the system design and focus the methodological assumptions used in the analysis. When applicable, adjustments to the design and analysis using collected empirical information were performed during the commissioning phase.

MATERIALS AND METHODS

A detailed description of the REMS design was arranged into subsystems and used to identify potential sources of measurement uncertainty. A comprehensive instrument error analysis described the best estimate of standard uncertainties for each measurement used to compute ER. Finally, measurement uncertainties were propagated to obtain uncertainties associated with ER calculation and used in a three-scenario sensitivity analysis with varied (but typical) gas analyzer and ventilation measurement accuracies.

REMS DESIGN AND SUBSYSTEMS

REMS was installed in six of twelve metabolism stalls at the University of Illinois at Urbana-Champaign Beef and Sheep Field Facility and consisted of four major subsystems: (1) six identical positive pressure ventilated hood chambers (VHC) with an internal volume of approximately 1100 L, capable of enclosing the head and neck of 230 to 1000 kg beef animals; (2) individual thermal environmental control subsystem (TECS) units used to condition recirculated air for comfort and humidity control for each VHC; (3) a fresh air supply and measurement subsystem (FASMS) to provide animal fresh air requirements and deliver precisely metered ventilation; and (4) a gas sampling subsystem (GSS) to collect gas samples from the chambers and the ventilation supply air (background) and to record the gas concentrations used in gas emission calculations.

A detailed schematic of the instrumentation and equipment for each component is provided in figure 1, and isometric views of the VHCs with TECS and FASMS components are shown in figure 2. The VHCs, FASMS, and GSS collection lines and pumps are housed in a controlled environment, while the personal computer and gas analyzer are

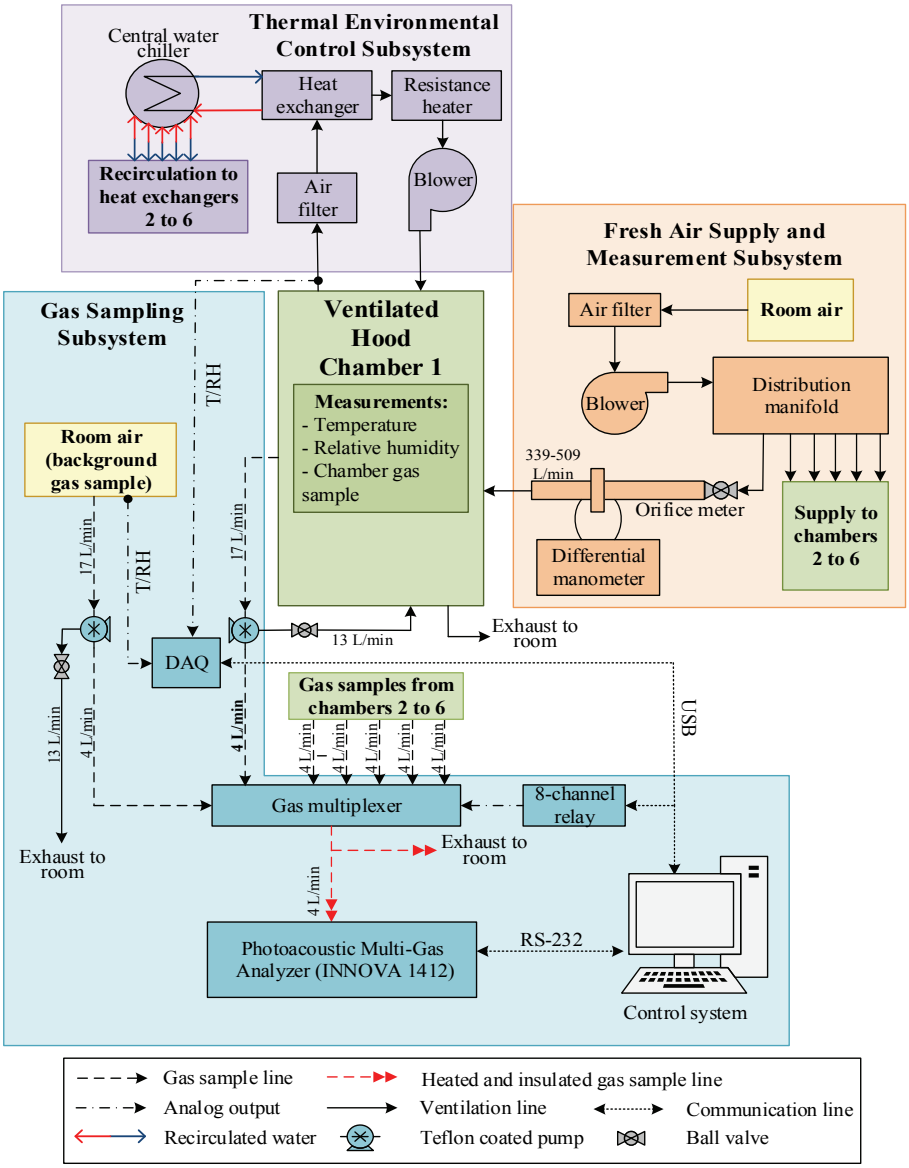

Figure 1. Schematic of the Ruminant Emission Measurement System (REMS) with a detailed subsystem breakdown for one ventilated hood chamber. Six identical chambers are part of the system, and each has an individual thermal environmental control subsystem (TECS) and fresh air supply and measurement subsystem (FASMS). The central water chiller in the TECS, the blower in the FASMS, and the gas sampling subsystem (GSS) are connected and integrated with the six chambers.

in an adjacent room (fig. 3). REMS also features an alarm system to alert operators in the event of high CO_2 levels (>9000 ppm_v) in order to protect operators, maintain animal welfare, and ensure data integrity.

Ventilated Hood Chambers

The six positively pressurized VHCs (fig. 4) were custom assembled to design specifications by ShapeMasters, Inc. (Ogden, Ill.). Each VHC featured transparent polycarbonate panels on the front, sides, top, and bottom. For the back (animal entrance), aluminum was used (fig. 2). The polycarbonate panels were secured in an aluminum frame (80/20, Inc., Columbia City, Ind.) for durability, reduced weight, animal comfort, and safety. Similar chamber design and construction have been reported elsewhere (Kelly et al., 1994; Place et al., 2011; Suzuki et al., 2007). Openings at the top were added for ventilation and gas sampling ports (fig. 2). On the front, a door with a foam tape seal allowed easy access to the removable feed bin (fig. 2). The inside of the chamber included a drinker (C20103N, Nasco, Inc., Fort Atkinson, Wisc.). Two larger circular holes (0.152 m) on top of the chamber accommodated the TECS recirculation supply and return connected via flexible, insulated 0.1016 m (4 in.) ducts. The FASMS inlet, GSS chamber gas sampling port, a hole for the drinker hose, and excess gas sample return were drilled in the top of the chamber (fig. 4b). Placement of the FASMS inlet and TECS recirculation return promoted the mixing of fresh air by entraining it into the recirculation supply air and using the recirculation return to pull air back to the top. Each chamber was mounted on four casters for moving the chamber into and out of the metabolism stall.

Figure 2. Isometric drawing of one ventilated hood chamber with thermal environmental control subsystem (TECS) and fresh air supply and measurement subsystem (FASMS) components. The gas sampling subsystem (GSS) is connected to the gas multiplexer and integrated with the other ventilated hood chambers (fig. 1).

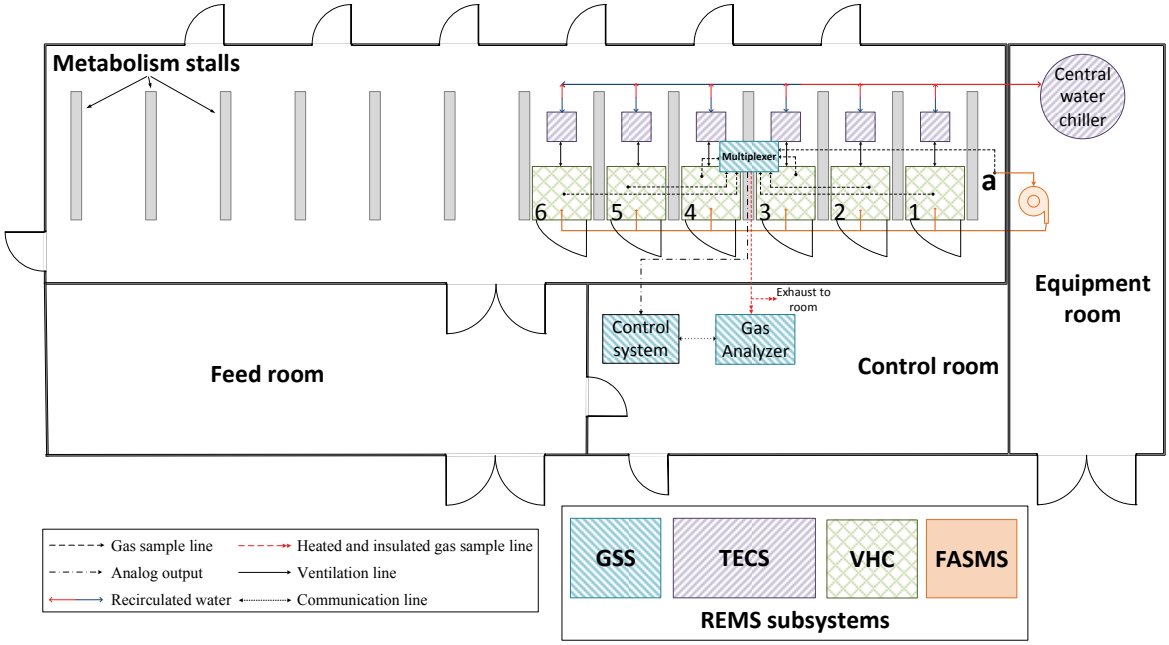

Figure 3. Layout of the ruminant emission measurement system with four major subsystems highlighted; "a" indicates the location of the background gas concentration, temperature, and relative humidity measurements that are supplied through the fresh air supply and measurement subsystem (FASMS).

The neck stanchion in the existing metabolism stalls was used to restrain the animal, and a zippered canvas hood with drawstring was secured around the animal's neck to enclose the space between the chamber opening and the animal's body. The hood was attached to the octagonal opening on the back of the chamber (fig. 4a) to minimize potential infiltration, which could affect emission calculations. The design allows the animal to stand or lie down for comfort while its head and neck remain inside the chamber.

Thermal Environmental Control Subsystem

The thermal environment inside the chamber was regulated by the TECS (figs. 1 to 3). Located above each chamber, a carefully sealed enclosure was made from 2.54 cm (1 in.) rigid foam polystyrene insulation. The enclosure housed a pleated air filter for dust removal, a 750 W electric resistance heater (model CSF00232, Tempco Electric Heater Corp., Wood Dale, Ill.), a blower (Dayton model 1TDR3) for air recirculation and to promote thorough gas

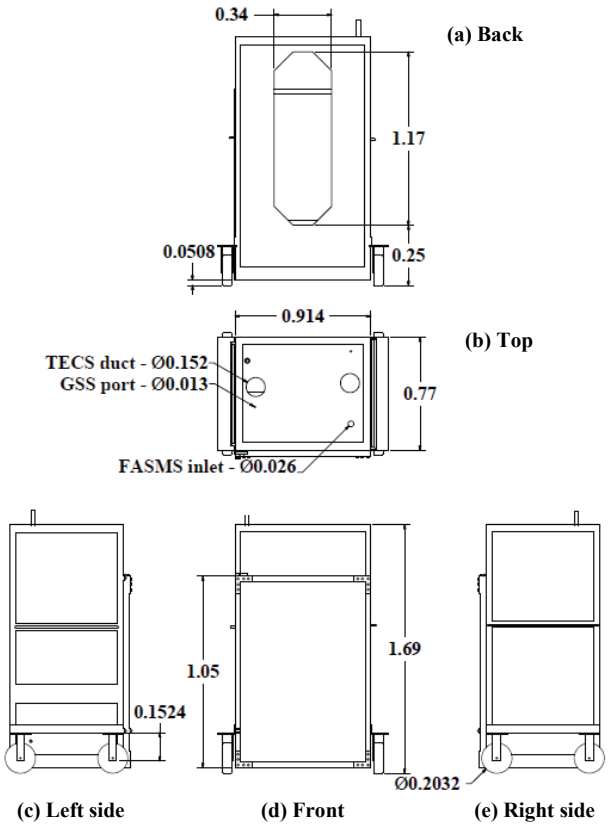

Figure 4. Plan views of the (a) back, (b) top, (c) left side, (d) front, and (e) right side of the ventilated hood chamber (all dimensions are in m). The animal's head and neck enter the chamber through the back. The top view shows inlets and ports for the fresh air supply and measurement subsystem (FASMS), thermal environmental control subsystem (TECS), and gas sampling subsystem (GSS).

mixing, and a 1 kW capacity (750 W sensible and 250 W latent heat) heat exchanger (cooling coil). The blower inside the enclosure recirculated air at a constant rate from the chamber through the filter, heat exchanger, and heater. Water vapor generated by the animal was continuously removed from the airstream by condensation at the heat exchanger. The six heat exchangers used supply and return manifolds to circulate chilled water from a central unit with a setpoint of 7.2°C (10.6 kW, Koolant Kooler SV3000-W, Dimplex Thermal Solutions, Kalamazoo, Mich.). The TECS was custom fabricated and installed by Polar Refrigeration, Heating, and Cooling, Inc. (Urbana, Ill.). Capacities for cooling and water vapor removal were estimated slightly beyond the anticipated maximum total heat production of a 1000 kg steer (Albright, 1990). A proportional temperature controller (C450CPN-1C, Johnson Controls, Inc., Milwaukee, Wisc.) connected to the heat source was programmed to operate between the temperature range of 26°C (heater off) and 16°C (heater on) within the heat exchange enclosure to maintain the desired temperature within the chamber. The programmed temperature range ensured thermoneutral conditions. Thermal control capacity requirements were substantially reduced by supplying the chambers with fresh air from the environmentally controlled barn (figs. 1 and 3).

Fresh Air Supply and Measurement Subsystem

The FASMS was uniquely designed to supply continuous fresh air and to positively pressurize the VHCs (figs. 1 to 3) independently of the TECS operation. Many reported applications of the chamber technique as either whole-body or ventilated hood-type used negatively pressurized chambers (Bhatta et al., 2007; Hellwing et al., 2012; McLean and Tobin, 1987; Pinares-Patiño and Waghorn, 2012; Place et al., 2011; Storm et al., 2012). The disadvantages of negatively pressurized chambers include potential unquantified air infiltration and subsequent dilution of gases in the chamber. In contrast, a positive pressure system has some advantages for gas sampling because chamber leaks occur outward (from the chamber to the room) and pose no risk of unmeasured outside air infiltration, which could result in gas sample dilution (Moody et al., 2008). This configuration prevents gas sample dilution even for leakages with high flow rates and avoids potential uncertainty (primarily as a bias) in emission calculations due to unquantifiable leakage or infiltration. A key requirement is to maintain positive pressure in the VHC to achieve these advantages.

Fresh air was supplied by a radial centrifugal blower (model PW11, Peerless Blowers, Hot Springs, N.C.) and distributed to all six chambers by a 7.62 cm (3 in.) PVC pipe manifold. A filter upstream of the blower prevented dust and other particles from contaminating the flowmeters. The ventilation and recirculation rates were selected to maintain detectable gas concentrations while sustaining acceptable equilibrium CO_2 levels in the chamber. Background gas samples (incoming ventilation air) for gas concentration, temperature, and relative humidity measurement were monitored at the inlet of the blower (in the room; fig. 3). The incoming volumetric flow rate for each chamber was measured with custom-made, individually calibrated orifice meters; a detailed description of their design, construction, calibration, and uncertainty analysis is reported elsewhere (Ramirez et al., 2013; Ramirez, 2014; Ramirez et al., 2014).

Gas Sampling Subsystem

The GSS (figs. 1 to 3) of REMS applied similar monitoring practices to those established for air emissions from feeding operations in the U.S. (Maia et al., 2012; Moody et al., 2008). The GSS was positively pressurized except from the gas sampling port in the chamber to the inlet on the vacuum side of pump, thereby reducing potential leakage between the VHC and the gas analyzer. A custom gas distribution multiplexer made of a solenoid array and relays controlled the switching between gas samples taken from each chamber and background sampling ports (Sun, 2013). Samples were routed to an infrared photoacoustic spectroscopy multi-gas analyzer (Innova model 1412, LumaSense Technologies, Inc., Santa Clara, Cal.) configured with CH_4, CO_2, N_2O, NH_3, and SF_6 optical filters. A polytetrafluoroethylene coated pump (model EW-79200-30, Cole-Parmer, Inc., Vernon Hills, Ill.) extracted gas samples at approximately 17 L min^{-1}, with 4 L min^{-1} routed to the gas analyzer and the remaining 13 L min^{-1} recirculated to the chamber. After passing through the gas analyzer, samples were exhausted to the room. Custom control system software de-

veloped in LabVIEW (ver. 8.2.1., National Instruments, Inc., Austin, Tex.) interfaced the multiplexer and gas analyzer for real-time monitoring of concentration and environmental conditions. When the control system received a serial input (RS-232) from the gas analyzer, a command to a USB 8-channel relay (USB-ERB08, Measurement Computing Corp., Norton, Mass.) sequentially opened each of the seven solenoid valves to direct flow from the sampling locations to the gas analyzer. Environmental parameters were also monitored and recorded by the control system with temperature and relative humidity sensors (HMP60-L, Vaisala, Helsinki, Finland) connected to a data acquisition card (USB-1608G Series, Measurement Computing Corp., Norton, Mass.).

For each gas sampling location (chambers and background), ten gas concentration measurements were taken for each of the five gases (CH_4, CO_2, N_2O, NH_3, and SF_6) at a customizable sampling interval dependent on the sample integration time (SIT) of each optical filter in the multi-gas analyzer. For the aforementioned configuration, the SITs were 5 s (CH_4), 1 s (CO_2), 1 s (N_2O), 5 s (NH_3), and 1 s (SF_6), thus requiring approximately 43 s per sample to complete (i.e., the gas analyzer sampling cycle when all five gases are monitored). From these ten serial gas samples, the first five were discarded (flushing), and the last five were used for analysis. This procedure followed gas sampling protocols developed to guarantee that the response time for each gas was reached (Moody et al., 2008; Maia et al., 2012; Sun, 2013).

EMISSION RATE CALCULATION

The REMS integrates measurements from numerous instruments to compute animal ER. The parameters from these measurements were incorporated into the mass flow balances of the system to derive ER. Moist air (total) and gas component mass flow balances were performed using the chamber as the control volume and assuming steady-state conditions.

Moist Air Mass Flow Balance

In the moist air mass flow balance (eq. 1), net animal moist air generation was assumed negligible; thus, the mass flow of incoming air equaled the mass flow leaving the chamber. Moist air density of the mixed air inside the chamber was derived from the measurable parameters of temperature, relative humidity, and barometric pressure using psychrometric equations (Albright, 1990). The moist air mass balance resulted in:

$$\dot{V}_{ex} = \dot{V}_{in} \times \left(\frac{\rho_{in}^{ma}}{\rho_{ch}^{ma}} \right) \tag{1}$$

where

$\dot{V}_{ex}$ = exhaust volumetric flow rate leaking out of the chamber ($m^3\ s^{-1}$)

$\dot{V}_{in}$ = incoming moist air ventilation volumetric flow rate ($m^3\ s^{-1}$)

ρ_{in}^{ma} = incoming moist air density ($kg_{da}\ m^{-3}$)

ρ_{ch}^{ma} = chamber exhaust moist air density ($kg_{da}\ m^{-3}$).

Gas Mass Flow Balance

The steady-state gas balance was obtained from the difference between the chamber exhaust gas mass flow ($\dot{m}_{ex}^{gas}$) and incoming gas mass flow ($\dot{m}_{in}^{gas}$) (fig. 5, eq. 2). The result of this difference provided the gas generation rate ($\dot{m}_{gen}^{gas}$).

Isolating for mass flow generated and incorporating measured parameters yields:

$$\dot{m}_{gen}^{gas} = \frac{\left(\dot{V}_{ex} \times C_{ch} \times \frac{M \cdot p_b}{R \cdot T_{ch}} \times 10^{-6} \right)}{\dot{m}_{ex}^{gas}} - \frac{\left(\dot{V}_{in} \times C_{in} \times \frac{M \cdot p_b}{R \cdot T_{in}} \times 10^{-6} \right)}{\dot{m}_{in}^{gas}} \tag{2}$$

where

$\dot{m}_{gen}^{gas}$ = generated gas mass flow ($g\ s^{-1}$)

C_{ch} = chamber gas concentration (ppm_v)

C_{in} = incoming background gas concentration (ppm_v)

T_{ch} = chamber dry-bulb temperature (K)

T_{in} = incoming background dry-bulb temperature (K)

M = molecular mass of gas ($g\ mol^{-1}$)

p_b = local barometric pressure (98.639 kPa; ASHRAE, 2013)

R = universal ideal gas constant (8.314 $m^3\ Pa\ K^{-1}\ mol^{-1}$).

The terms $\frac{M \cdot p_b}{R \cdot T_{ch}} \times 10^{-6}$ and $\frac{M \cdot p_b}{R \cdot T_{in}} \times 10^{-6}$ convert ppm_v (volumetric concentration) into $g\ m^{-3}$ (absolute units) at the measured conditions. Exhaust gas mass flow is comprised of the exhaust ventilation rate and the concentration of the mixed chamber gas; however, exhaust ventilation rates cannot be measured directly because positive pressure leakages occur in several parts of the chamber (outward direction). Exhaust ventilation rate was determined from other direct measurements after manipulation of measurable parameters (eq. 1). The result of the gas mass flow balance expressed in terms of measureable parameters was obtained with the substitution of equation 1 into equation 2 and simplifying:

$$\mathrm{ER} = \dot{m}_{gen}^{gas} = \dot{V}_{in} \left(\frac{\rho_{in}^{ma}}{\rho_{ch}^{ma}} \frac{C_{ch}}{T_{ch}} - \frac{C_{in}}{T_{in}} \right) \times 10^{-6} \left(\frac{M \cdot p_b}{R} \right) \tag{3}$$

where ER is the animal emission rate derived from the

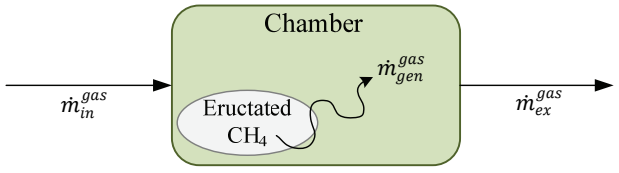

Figure 5. Gas component mass balance diagram. The generated gas represented is methane, although any gas can be used.

mass balance (g s^{-1}).

The accumulated emission (E, g) is obtained from the integration of the emission rates (eq. 3) over the length of the experiment:

$$E = \sum_{i=1}^{n-1} \frac{1}{2}\left(t_{i+1} - t_i\right) \times \left(\mathrm{ER}_i + \mathrm{ER}_{i+1}\right) \quad (4)$$

where

E = accumulated emission while the animal is monitored in the chamber (g)

n = number of emission rate measurements

t = elapsed time (s).

EMISSION STANDARD UNCERTAINTY

The absolute standard uncertainty (denoted by Δ) associated with the computed ER (eq. 4) is a statistically based approximation of measurement error obtained from the root-sum-square (RSS) of measurement uncertainty sources, which are represented by the parameters in equation 3 (ISO, 2008; Taylor and Kuyatt, 1994). Barometric pressure, molecular mass, and the universal ideal gas constant were determined to have negligible standard uncertainty; thus, they were excluded from the analysis. The physical relationships between measurements and ER (sensitivity coefficients) are signified by the partial derivatives (Taylor and Kuyatt, 1994). A truncated first-order Taylor series approximation, applied to equation 3, assuming independent measurements, was used to determine ΔER (Gates et al., 2009; ISO, 2008):

$$\Delta \mathrm{ER} = \sqrt{\begin{aligned} &\left(\frac{\partial \mathrm{ER}}{\partial \dot{V}_{in}} \Delta \dot{V}_{in}\right)^2 \\ &+\left(\frac{\partial \mathrm{ER}}{\partial T_{in}} \Delta T_{in}\right)^2 + \left(\frac{\partial \mathrm{ER}}{\partial T_{ch}} \Delta T_{ch}\right)^2 \\ &+\left(\frac{\partial \mathrm{ER}}{\partial \rho_{in}^{ma}} \Delta \rho_{in}^{ma}\right)^2 + \left(\frac{\partial \mathrm{ER}}{\partial \rho_{ch}^{ma}} \Delta \rho_{ch}^{ma}\right)^2 \\ &+\left(\frac{\partial \mathrm{ER}}{\partial C_{in}} \Delta C_{in}\right)^2 + \left(\frac{\partial \mathrm{ER}}{\partial C_{ch}} \Delta C_{ch}\right)^2 \end{aligned}} \quad (5)$$

where

ΔER = expected RSS error of the combined absolute standard uncertainty (g s^{-1})

$\Delta \dot{V}_{in}$ = incoming moist air ventilation absolute standard uncertainty (m^3 s^{-1})

ΔT_{in} = incoming dry-bulb temperature absolute standard uncertainty (K)

ΔT_{ch} = chamber dry-bulb temperature absolute standard uncertainty (K)

$\Delta \rho_{in}^{ma}$ = incoming moist air density absolute standard uncertainty (kg_{da} m^{-3})

$\Delta \rho_{ch}^{ma}$ = chamber moist air density absolute standard uncertainty (kg_{da} m^{-3})

ΔC_{in} = incoming gas concentration absolute standard uncertainty (ppm_v)

ΔC_{ch} = chamber gas concentration absolute standard uncertainty (ppm_v).

Relative standard uncertainty (%ΔER) was expressed as 100 × (ΔER/ER), i.e., percent of measured value.

The standard uncertainty (ΔE, g) associated with the accumulated emission (eq. 6) is the standard uncertainty associated with each ER computation, integrated over the length of the experiment:

$$\Delta E = \sqrt{\sum_{i=1}^{n-1} \left(\frac{1}{2}\left(t_{i+1} - t_i\right) \times \left(\Delta \mathrm{ER}_i + \Delta \mathrm{ER}_{i+1}\right) \right)^2} \quad (6)$$

where ΔE is the standard uncertainty of accumulated emission while the animal is monitored in the chamber (g).

Parameter Standard Uncertainty

Uncertainty sources considered for each parameter were associated with the instrumentation involved in the measurement, including instrument resolution, repeatability, calibration reference standard error, other calibration parameters, and the manufacturer's traceable and non-traceable accuracy. A normal error distribution (divisor = 1) and rectangular error distribution (divisor = √3) were applied accordingly (Taylor and Kuyatt, 1994). The following discussion describes the methods used to determine parameter uncertainties from equation 5.

A detailed uncertainty analysis for the parameters and instruments in the FASMS was provided in previous work (Ramirez, 2014; Ramirez et al., 2014). The standard uncertainties of temperature and relative humidity were determined from the manufacturer's non-traceable accuracy, and moist air density standard uncertainty was quantified from the partial derivative of density with respect to temperature and relative humidity. Incoming ventilation rate standard uncertainty was dependent on differential pressure measurement standard uncertainty, moist air density standard uncertainty, linear regression slope standard error, and standard error of inverse prediction (Ramirez et al., 2014).

Incoming and exhaust concentration standard uncertainties measured with the gas analyzer were estimated from five sources (eq. 7). The first source was obtained from a post-calibration repeatability test using a primary certified CH_4 gas cylinder (500 ppm_v). Instrument repeatability was checked after calibration at ideal instrument operation conditions and was obtained from the standard deviation of 13 readings. The second source was from the primary certified tolerance (PCT), which is the CH_4 primary certified reference used to calibrate the gas analyzer (±1% of the certified value). The remaining three uncertainty sources were based on manufacturer's information. These included repeatability (REPI), range drift (RD), and resolution (RES). Resolution was assumed to be half of the practical CH_4 optical filter detection limit. The practical detection limit followed manufacturer's recommendations, taken as 10-fold greater than the theoretical detection limit provided in the specifications for a sample integration time of 5 s. The detection limits of other gases were SF_6 = 0.006 ppm_v, CO_2 = 5 ppm_v, N_2O = 0.03 ppm_v, and NH_3 = 0.2 ppm_v. The

five sources of standard uncertainties combined produced:

$$\Delta C_i = \sqrt{\left(\frac{\text{SDPC}}{1}\right)^2 + \left(\frac{\text{REPI}\cdot C_i}{\sqrt{3}}\right)^2 + \left(\frac{\text{PCT}\cdot\text{AC}}{\sqrt{3}}\right)^2 + \left(\frac{\text{RD}\cdot C_i}{\sqrt{3}}\right)^2 + \left(\frac{\text{RES}}{\sqrt{3}}\right)^2} \quad (7)$$

where

ΔC_i = gas concentration combined standard uncertainty (ppm_v)

i = *in* for incoming air or *ch* for chamber

SDPC = standard deviation (n = 13) of post-calibration repeatability (±1%, ppm_v, normal distribution)

REPI = instrument repeatability from manufacturer (±1%, ppm_v, rectangular distribution)

PCT = primary certified tolerance (±1% of AC, ppm_v, rectangular distribution)

AC = actual concentration from manufacturer of primary certified tank (499.9 ppm_v)

RD = range drift for measured gas concentration (±2.5% for three months, ppm_v, rectangular distribution)

RES = instrument resolution = (10 × DL)/2 (rectangular distribution)

DL = detection limit for CH_4 (0.4 ppm_v, rectangular distribution).

Uncertainty Contributions and Expanded Uncertainty

The contribution of each parameter in equation 5 to ΔER is the product of the sensitivity coefficient and the standard uncertainty of the input quantity (eq. 8):

$$C_a = 100 \times \frac{\left(\frac{\partial \text{ER}}{\partial a}\Delta a\right)^2}{(\Delta \text{ER})^2} \quad (8)$$

where

a = individual parameters (error source)

C_a = contribution of an individual parameter a on a percent basis (%)

Δa = absolute standard uncertainty associated with an individual parameter

$\partial \text{ER}/\partial a$ = sensitivity coefficient associated with the uncertainty of each individual parameter.

Expanded ΔER was determined by applying a coverage factor k (expanded ΔER = k × ΔER). The value of k is a function of the ER effective degrees of freedom and the confidence level assumed for the uncertainty source. The effective degrees of freedom (df_{eff}^{ER}) was obtained with the Welch-Satterthwaite formula (eq. 9; ISO, 2008; Taylor, 2009). The value of k was calculated for an approximate confidence level of 95%:

$$df_{eff}^{\text{ER}} = \frac{(\Delta \text{ER})^4}{\sum \frac{\left(\frac{\partial \text{ER}}{\partial a}\Delta a\right)^4}{df_a}} \quad (9)$$

where

df_{eff}^{ER} = ER effective degrees of freedom

df_a = degrees of freedom associated with an individual parameter a.

The error distribution associated with each error source (Δa) affects the assumptions for df_a. For this study, two types of error distribution were used: (1) normal distribution, which belongs to a class of Type A error, and (2) rectangular distribution, which is assumed to be a Type B error (ISO, 2008; Taylor and Kuyatt, 1994). Type B errors are assumed to have large degrees of freedom ($df_a \to \infty$), in which case they do not affect df_{eff}^{ER} calculations because they force their denominator terms to zero:

$$\lim_{df_a \to \infty} \frac{\left(\frac{\partial \text{ER}}{\partial a}\Delta a\right)^4}{df_a} = 0$$

Degrees of freedom (df_a) from parameters with normal distributions were applied to equation 9 to determine df_{eff}^{ER}. A *t*-distribution was used to determine the coverage factor at a 95% confidence level (ISO, 2008; Taylor and Kuyatt, 1994). The calculation of df_{eff}^{ER} is provided in the following section.

Coverage Factor Verification

A k factor of 2 to denote a 95% level of confidence was determined from the analysis of effective degrees of freedom (eq. 9) for the two largest Type A uncertainty contributions: (1) SDPC (eq. 7), associated with concentration measurements in the GSS, and (2) the standard error of the inverse prediction (SE(IP)), which is an uncertainty associated with the orifice meter calibration in the FASMS (Ramirez et al., 2014). SDPC contributed <27% of the ventilation uncertainty, with the remaining uncertainty (≈73%) belonging to Type B errors. Similarly, SE(IP) contributed to less than 1% of the total FASMS uncertainty; more than 98% of the FASMS uncertainty was associated with the pressure transducer device, which is a Type B error source. Effective degrees of freedom for ventilation, concentration, and emission rate were determined using scenario 1 (table 1, for C_{ch} = 500 ppm_v). All df_{eff} values were much greater than 30, which corresponds to k = 2 at a 95% confidence level.

Sensitivity Analysis with Three Scenarios

A sensitivity analysis was performed to assess the effects of each ER input parameter (table 2) on ΔER and %ΔER under three scenarios. Parameters set as constants for all three scenarios included incoming concentration (C_{in} = 20 ppm_v, CH_4), incoming temperature (T_{in} = 20°C), chamber temperature (T_{ch} = 22°C), incoming moist air density (ρ_{in}^{ma} = 1.17 kg m^3), and chamber moist air density

Table 1. Effective degrees of freedom for ventilation ($df_{eff}^{\dot{V}_{in}}$), concentration ($df_{eff}^{C_{ch}}$), and emissions rate (df_{eff}^{ER}) calculated from Type A errors.

	Ventilation[a]	Concentration[b]	Emission Rate
df_{eff} (eq. 9)	$df_{eff}^{\dot{V}_{in}} = \frac{(\Delta \dot{V}_{in})^4}{\frac{(SE(IP))^4}{df_{SE(IP)}}}$	$df_{eff}^{C_{ch}} = \frac{(\Delta C_{ch})^4}{\frac{(SDPC)^4}{df_{SDPC}}}$	$df_{eff}^{ER} = \frac{(\Delta ER)^4}{\frac{\left(\frac{\partial ER}{\partial \dot{V}_{in}}\Delta \dot{V}_{in}\right)^4}{df_{eff}^{\dot{V}_{in}}} + \frac{\left(\frac{\partial ER}{\partial C_{ch}}\Delta C_{ch}\right)^4}{df_{eff}^{C_{ch}}}}$
df_{eff} values	6.22E+08	74	812
k factor[c]	1.960	1.997	1.960

[a] SE(IP) = 0.1604 L min^{-1}; df_{SE} = 18 (Ramirez et al., 2014).
[b] SDPC = 1% of measured value = 5 ppm$_v$; df_{SDPC} = 12.
[c] Determined from a t-distribution table (ISO, 2008).

Table 2. Summary of parameters from instrument error analysis contributing to equation 4 used to determine standard uncertainty associated with animal emissions. Sources of uncertainty from each measurement were unique, thus requiring individual characterization.

Symbol	Unit	Description	Uncertainty Source	Manufacturer	Reference
ΔT_{in}, ΔT_{ch}	K	Dry-bulb temperature	T/RH sensor	HMP60-L, Vaisala, Helsinki, Finland	Ramirez et al., 2014
ΔRH_{in}, ΔRH_{ch}	%	Relative humidity	T/RH sensor	HMP60-L, Vaisala, Helsinki, Finland	Ramirez et al., 2014
$\Delta \dot{V}_{in}$	m^3 s^{-1}	Incoming flow rate	Orifice meter	Custom	Ramirez et al., 2014
ρ_{in}^{ma}, ρ_{ch}^{ma}	kg m^{-3}	Moist air density	Albright, 1990 (equation 2-16)	-	Ramirez et al., 2014
ΔC_{in}, ΔC_{ch}	ppm$_v$	Gas concentration	Infrared photoacoustic multi-gas analyzer	Innova 1412, LumaSense Technologies, Inc., Santa Clara, Cal.	Equation 7

(ρ_{ch}^{ma} = 1.16 kg m^{-3}) (table 3).

For scenario 1, eleven levels of CH_4 concentrations were used (C_{ch} = 50, 75, 100, 200, 300, 400, 500, 600, 700, 800, and 900 ppm$_v$), encompassing an ER range from 0.6 to 17.2 g h^{-1}, which follows a baseline for cattle CH_4 emission found in the literature (Place et al., 2011). Ventilation rate and standard uncertainties were set as constants ($\dot{V}_{in}$ = 500 and 12.32 L min^{-1}, respectively). In scenario 2, incoming CH_4 concentration (C_{in} = 20 ppm$_v$) and chamber gas concentrations (the same 11 levels used in scenario 1) were tested for five levels of relative standard uncertainty (%ΔC_{in} = %ΔC_{ch} = 1%, 2.5%, 5%, 7.5%, and 10%). Ventilation rate and standard uncertainties were set as constants and assumed to have the same values used in scenario 1. Finally, in scenario 3, ventilation rate relative uncertainty was tested for five levels (%$\dot{V}_{in}$ = 1%, 2.5%, 5%, 7.5%, and 10%) against the same 11 levels of CH_4 concentrations applied to scenarios 1 and 2. This represents a scenario in which the ventilation rate remained constant but ventilation rate standard uncertainty increased (i.e., loss of accuracy due to instrument drifts) (table 3). Note that concentration uncertainties varied with input concentrations for all three scenarios because these uncertainties are a function of the concentration input value.

RESULTS AND DISCUSSION

Results of the ER sensitivity analysis for three scenarios (table 3) are summarized below. Unless otherwise stated, all uncertainties associated with ER are expressed as the expanded standard uncertainty with a coverage factor of 2 (k = 2), corresponding to an approximately 95% level of confidence.

Table 3. Parameter values and associated standard uncertainties, absolute (Δ) and relative (%Δ), used in the sensitivity analysis. Scenario 1 simulated expected operation of the REMS, while scenarios 2 and 3 simulated relative standard uncertainty changes in concentration and ventilation measurements, respectively, at 1%, 2.5%, 5%, 7.5%, and 10%

			Parameter Standard Uncertainty					
			Scenario 1		Scenario 2		Scenario 3	
Input	Value[a]	Unit	Δ	%Δ	Δ	%Δ	Δ	%Δ
Concentration	C_{in} = 20 C_{ch}[b]	ppm$_v$	0.4 Varied[c]	1.9 Varied[b]	0.4 Varied[c]	Varied[d] Varied[d]	0.4 Varied[b]	1.9 Varied[b]
Ventilation	$\dot{V}_{in}$ = 500	L min^{-1}	12.32	2.46	12.32	2.46	Varied[c]	Varied[d]
Temperature	T_{in} = 20 T_{ch} = 22	°C	0.5 0.5	2.5 2.3	0.5 0.5	2.5 2.3	0.5 0.5	2.5 2.3
Air density	ρ_{in}^{ma} = 1.17 ρ_{ch}^{ma} = 1.16	kg m^{-3}	0.003 0.003	0.2 0.2	0.003 0.003	0.2 0.2	0.003 0.003	0.2 0.2
Constants	Pressure[e]	p_b = 98,639 Pa						
	Gas constant	R = 8.31462 m^3 Pa K^{-1} mol^{-1}						
	Molar mass	M_{CH4} = 16.04 g mol^{-1}						

[a] in = background and ch = mixed chamber gas.
[b] Methane state point range was 50, 75, 100, 200, 300, 400, 500, 600, 700, 800, and 900 ppm$_v$ for expected animal CH_4 generation.
[c] Absolute and relative uncertainty is a function of input value.
[d] Absolute uncertainty determined from simulated relative uncertainty.
[e] Local barometric pressure (Savoy, Ill.).

SCENARIO 1

In scenario 1 (figs. 6 and 7, table 4), expanded ΔER linearly increased with CH_4 emissions, and expanded %ΔER exponentially decreased to a constant value (fig. 6). Expanded %ΔER values were lowest (≈6%) for higher CH_4 emission rates (ER >3.5 g h^{-1}; CH_4 concentrations >200 ppm_v) and greater (6% to 13%) for lower CH_4 emission rates (ER <3.5 g h^{-1}; CH_4 concentrations <200 ppm_v), which can be explained by the increase in contribution of the background concentration measurement when the chamber concentration was in the lower range (fig. 7). Expanded %ΔER was stable (≈6%) for CH_4 emission rates >3.5 g h^{-1} (CH_4 concentrations >200 ppm_v).

Methane concentration and ventilation rate measurements had the largest role in ER uncertainty (fig. 7). The combination of incoming and chamber moist air density and temperature contributed less than 2% of the ER uncertainty for all ER values (table 4). Temperature and moist air density standard uncertainties were <3% and <1%, respectively. Ventilation rate contribution to ER uncertainty increased from 14% to 70% as ER and CH_4 concentration increased. Conversely, the contribution of the chamber concentration to ER uncertainty decreased from 49% to 29% as ER increased. Similarly, background concentration contribution to ER uncertainty decreased from 36% to <1% as ER increased. Scenario 1 provides insight into the effect of primary parameters (concentration and ventilation) on ER uncertainty. Because the uncertainty of these two parameters has the greatest effect on ER uncertainty, carefully controlling them can substantially improve ER estimates.

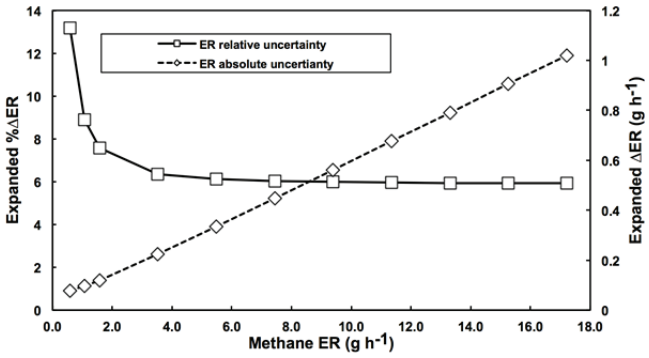

Figure 6. Scenario 1: Methane expanded ΔER and %ΔER for 11 levels of ER. The 11 levels correspond to a CH_4 concentration range of 50 to 900 ppm_v (0.6 to 17.2 g CH_4 h^{-1}).

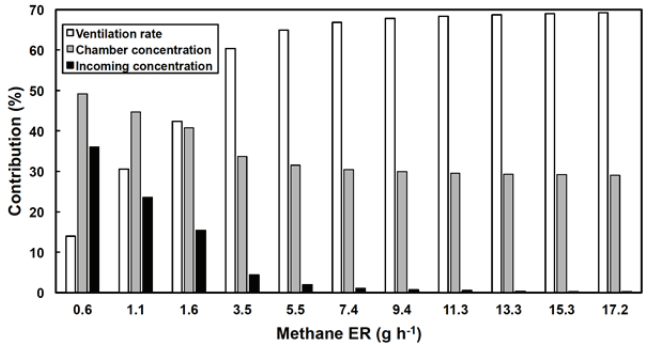

Figure 7. Contribution of three major sources to ER expanded uncertainty (scenario 1). Other sources were omitted for clarity but are summarized in table 4.

Table 4. Scenario 1: Summary of absolute (Δ) and relative (%Δ) standard uncertainties of the parameters contributing to ER expanded uncertainty for two simulation levels of CH_4 concentration (50 and 500 ppm_v).

			Scenario 1		
			Uncertainty		Contribution
Parameter[a]	Value	Unit	Δ	%Δ	(%)
ER	0.6	g h^{-1}	0.08[b]	13.3[b]	-
C_{ch}	50.0	ppm_v	1.4	2.8	49.2
C_{in}	20.0	ppm_v	1.2	6.0	36.0
$\dot{V}_{in}$	500.0	L min^{-1}	12.3	2.5	14.0
T_{ch}	22.0	°C	0.5	2.3	0.2
T_{in}	20.0	°C	0.5	2.5	2.9E-02
ρ_{ch}^{ma}	1.16	kg m^{-3}	2.7E-03	0.2	0.3
ρ_{in}^{ma}	1.17	kg m^{-3}	2.5E-03	0.2	0.3
ER	9.4	g h^{-1}	0.56[b]	6.0[b]	-
C_c	500.0	ppm_v	7.9	1.6	29.9
C_{in}	20.0	ppm_v	1.2	6.0	0.7
$\dot{V}_{in}$	500.0	L min^{-1}	12.3	2.5	67.8
T_{ch}	22.0	°C	0.6	2.7	0.3
T_{in}	20.0	°C	0.6	3.0	3.0E-02
ρ_{ch}^{ma}	1.16	kg m^{-3}	2.6E-03	0.2	0.6
ρ_{in}^{ma}	1.17	kg m^{-3}	2.6E-03	0.2	0.6

[a] ER is defined in equation 3.
[b] Expanded standard uncertainty with applied coverage factor of $k = 2$ (95% confidence).

SCENARIO 2

In scenario 2, as CH_4 emission rate increased, expanded %ΔER decreased until it became constant for ER >3.5 g h^{-1} (CH_4 concentrations >200 ppm_v) (fig. 8 and table 5). For CH_4 emission rates <3.5 g h^{-1} (CH_4 concentrations <200 ppm_v) and gas analyzer uncertainty >1%, expanded %ΔER values were variable until they reached a plateau (fig. 8). In the plateau phase (CH_4 emission rate >3.5 g h^{-1} and CH_4 concentrations >200 ppm_v), gas analyzer uncertainties were

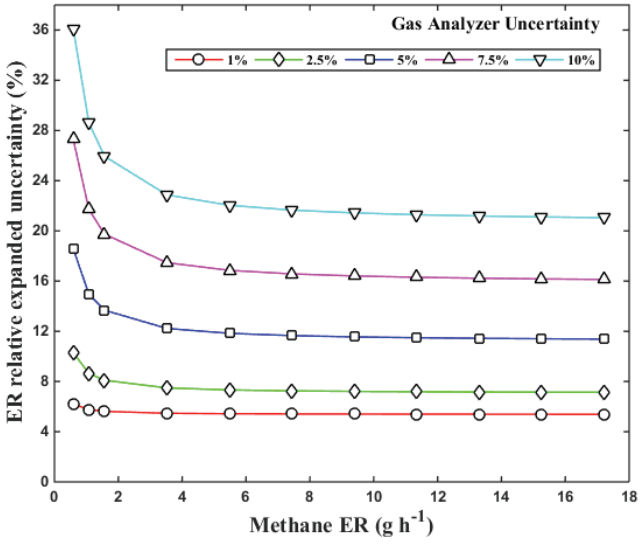

Figure 8. Scenario 2: methane concentration measurement uncertainties were held constant at 1%, 2.5%, 5%, 7.5%, and 10%. All other values are listed in table 5. The plot shows that gas analyzer relative expanded uncertainty increased as ER relative expanded uncertainty increased.

Table 5. Scenarios 2 and 3: Absolute (Δ) and relative (%Δ) standard uncertainties for the three major measurements and their contributions to ER expanded uncertainty. In scenario 2, gas analyzer uncertainty was 1% or 5%. In scenario 3, ventilation uncertainty was 1% or 5%. Two levels of CH_4 concentration (50 and 500 ppm_v) were chosen as an example.

			Scenario 2			Scenario 3		
			Uncertainty		Contribution	Uncertainty		Contribution
Parameter[a]	Value	Unit	Δ	%Δ	(%)	Δ	%Δ	(%)
ER	0.6	g h^{-1}	0.04[b]	6.2[b]	-	0.07[b]	12.4[b]	-
C_{ch}	50.0	ppm_v	0.5	1.0	28.6	1.4	2.8	55.7
C_{in}	20.0	ppm_v	0.2	1.0	4.5	1.2	6.0	40.7
$\dot{V}_{in}$	500.0	L min^{-1}	12.3[b]	2.5	63.0	5.0	1.0	2.6
ER	9.4	g h^{-1}	0.5[b]	5.4[b]	-	0.4[b]	3.9[b]	-
C_{ch}	500.0	ppm_v	5.0	1.0	14.9	7.9	1.6	69.0
C_{in}	20.0	ppm_v	0.2	1.0	0.0	1.2	6.0	1.6
$\dot{V}_{in}$	500.0	L min^{-1}	12.3[b]	2.5	83.2	5.0	1.0	25.8
ER	0.6	g h^{-1}	0.1[b]	18.6[b]	-	0.09[b]	15.8[b]	-
C_{ch}	50.0	ppm_v	2.5	5.0	79.9	1.4	2.8	34.3
C_{in}	20.0	ppm_v	1.0	5.0	12.7	1.2	6.0	25.1
$\dot{V}_{in}$	500.0	L min^{-1}	12.3[b]	2.5	7.0	25.0	5.0	40.0
ER	9.4	g h^{-1}	1.1[b]	11.6[b]	-	1.0[b]	10.6[b]	-
C_{ch}	500.0	ppm_v	25.0	5.0	81.3	7.9	1.6	9.6
C_{in}	20.0	ppm_v	1.0	5.0	0.1	1.2	6.0	0.2
$\dot{V}_{in}$	500.0	L min^{-1}	12.3[b]	2.5	18.2	25.0	5.0	89.7

[a] ER is defined in equation 3.
[b] Expanded standard uncertainty with applied coverage factor of $k = 2$ (95% CI).

1%, 2.5%, 5%, 7.5%, and 10%, which corresponded to expanded %ΔER of 5.4%, 7.1%, 11.4%, 16.1%, and 21.1%, respectively.

The contribution of the ventilation rate uncertainty to ER uncertainty (table 5) decreased as gas analyzer uncertainty increased. For CH_4 concentrations >200 ppm_v, the lower and upper limits of the gas analyzer contribution were 16% and 94%, respectively, which correspond to a ventilation contribution with upper and lower limits of 84% and 5%, respectively. When gas analyzer uncertainty was at its lowest (1%), gas analyzer contribution to ER uncertainty was about 16%, and ventilation rate contribution was about 84%. Conversely, when gas analyzer uncertainty was at its highest (10%), ventilation rate contribution was about 5%, while exhaust concentration measurement was 94%. The combination of incoming and exhaust moist air density and temperature contributed less than 2% to ER uncertainty for all ER values and the range of gas analyzer uncertainty values.

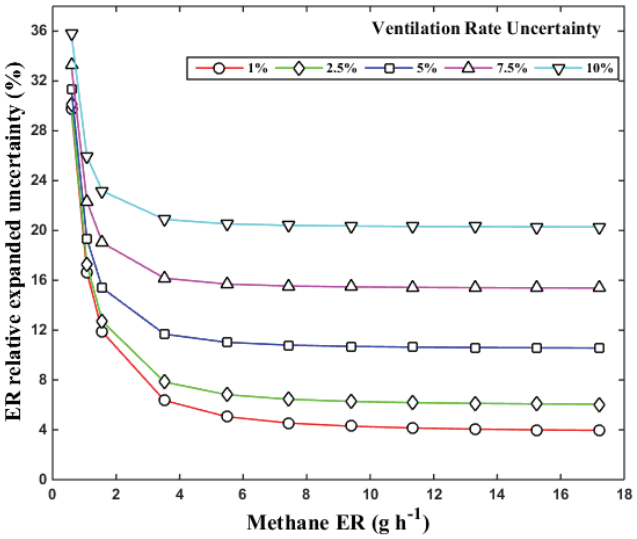

Figure 9. Scenario 3: ventilation rate uncertainty was held constant at 1%, 2.5%, 5%, 7.5%, and 10%. All other values are listed in table 5. The plot shows that ventilation relative uncertainty increased as ER relative expanded uncertainty increased.

SCENARIO 3

In scenario 3, as methane ER increased, expanded %ΔER decreased for all simulated ventilation rate uncertainties until they reached a plateau for ER >3.5 g h^{-1} (fig. 9). In addition, as ventilation rate uncertainty increased, expanded %ΔER increased. For CH_4 emission rates <3.5 g h^{-1} (CH_4 concentrations <200 ppm_v), expanded %ΔER values were variable until they reached a plateau for all simulated ventilation rate uncertainties (fig. 9). In the plateau phase, where CH_4 emission rates were >3.5 g h^{-1} (CH_4 concentrations >200 ppm_v), expanded %ΔER increased (3.8%, 5.9%, 10.5%, 15.4%, and 20.3%) with the increase in simulated ventilation rate uncertainties (1%, 2.5%, 5%, 7.5%, and 10%, respectively).

In terms of individual instrument uncertainty contributions, the gas analyzer uncertainty contribution (eq. 5) decreased as ventilation rate uncertainty increased. At CH_4 emission rates >3.5 g h^{-1} (CH_4 concentrations >200 ppm_v), the highest and lowest values of the gas analyzer contribution to the ER uncertainty were 98% to 2.5%, respectively, which corresponds to a ventilation contribution of 2.6% and 97%, respectively. For the lowest ventilation rate uncertainty (1%), the gas analyzer contribution was about 95% and the ventilation rate contribution was 4.2%. Conversely, for the highest ventilation rate uncertainty (10%), the gas analyzer contribution was about 2.5% and the ventilation rate contribution was about 97%. The combination of incoming and chamber moist air density and temperature contributed less than 2% of the ER uncertainty for all state points and gas analyzer scenarios.

Scenarios 2 and 3 provide insight into how uncertainty in concentration and ventilation rate measurements affects

the ER uncertainties. Uncertainty may increase from uncalibrated instrument drift or from using a less accurately calibrated instrument. Several factors affect instrument uncertainty. For instance, the fresh air source can have a significant impact on instrumentation uncertainty, such as unfiltered air degrading the orifice of pressure differential flowmeters. In addition, this analysis also assumes a non-zero background CH_4 concentration in the ventilation, which is important because many chamber systems are installed in barns or other buildings housing additional animals that may cause variations in the CH_4 concentration present in the chamber air supply. Similarly, the use of positive pressure systems helps eliminate background CH_4 from entering the chamber or gas sampling system. Neglecting background concentration may overpredict animal emissions, which is dependent on the relative magnitude of background and chamber concentrations. Neglecting air density, including fluctuations from the ventilation to the chamber, can also result in emission overpredictions.

The identification of the individual contributions relative to ER uncertainty is also important for instrument selection and maintenance. An increase in ventilation rate uncertainty can cause substantial impacts on the ER uncertainty. Instruments with low drift, that are easy to calibrate, and that are not affected by frequent changes in environmental conditions will reduce potential increases in ER uncertainty. Awareness of these factors can lead to improved experimental design and measurement system implementation. Frequent verification of the accuracy of key instrumentation (i.e., gas analyzers and flowmeters) can reduce uncertainty increases over time.

Knowledge of the methane ER uncertainty provides insight into the amount of confidence in the measurement system. Quantifying the combined uncertainty is essential for all respiration chambers and indirect calorimeters because reported values will carry standard uncertainties associated with each measurement. In addition, quantifying the combined uncertainty is imperative for determining the level of sensitivity needed to detect differences between experimental treatments (e.g., diets, mitigation strategies, etc.). Two computed values of CH_4 emission rate are significantly different if that difference lies outside the combined uncertainty of each CH_4 emission rate computation, assuming other random sources of error are assessed and systematic errors are estimated. Thus, combined uncertainty must be determined and reported. The determined combined uncertainty from design analysis should be subsequently applied to the system commissioning along with the assessment of systematic errors. Although the results presented here are applied to REMS, the presented methodology can, and should, be applied to other systems designed to quantify gas emissions.

SUMMARY AND CONCLUSIONS

REMS is an open-circuit respiration system comprising six positive pressure ventilated hood-type chambers for measuring beef cattle CH_4 emissions. The design features a unique positive pressure ventilation system for minimizing infiltration and subsequent gas measurement error by dilution. Uncertainties in REMS are shown to depend on instrument type and resolution, measurement reproducibility, calibration reference standard error and other calibration parameters, traceable and non-traceable manufacturer's accuracy, and assumptions regarding instrument error distributions. Emission rate standard uncertainty was determined by propagating the standard uncertainty derived for each instrument into the ER root-sum-square error.

Methane expanded $\%\Delta ER$ was approximately constant at ≈6% for ER >3.5 g h^{-1} (CH_4 concentrations >200 ppm_v). In addition, contributions to ER uncertainty were 29% from the gas analyzer and 69% from the ventilation rate. Other input measurements had negligible contributions. Increases in uncertainty associated with ventilation rate and gas concentration measurement have significant impact on ER standard uncertainty; thus, these instruments should have the lowest reasonable standard uncertainty, and emphasis should be given to calibration and accuracy verification.

REMS can potentially increase knowledge of what drives CH_4 production and ER in ruminants, particularly if REMS capabilities are used to investigate CH_4 production factors. REMS is uniquely qualified to accurately measure gas production from cattle, which is a key first step in understanding metabolic activity in cattle production and establishing possible mitigation strategies for environmental emissions.

A systematic approach to evaluate component measurement errors, such as conducted in this work, provides an estimate of the standard uncertainty of complex emission measurement systems and allows researchers to report animal emissions with a stated standard uncertainty. The analysis presented in this study can be extended to other systems measuring methane because it applies equally to any other open-circuit respiration chambers or indirect calorimeters computing quantities from several measurement inputs. In conclusion, a comprehensive uncertainty analysis should be a requirement in any gas measurement system design, and the present study is a major step in that direction.

ACKNOWLEDGEMENTS

This research was supported with funding provided by the Dudley Smith Initiative, University of Illinois College of ACES, and the Office of Research, University of Illinois College of ACES. The authors would like to acknowledge the contributions of research specialist Jingwei Su, graduate student Yi Sun, and undergraduate students Kellie Kroscher and Patricia Paulausky during the preparation and completion of this work.

REFERENCES

Albright, L. D. (1990). *Environment Control for Animals and Plants.* St. Joseph, Mich.: ASAE.

ASHRAE. (2013). Chapter 1: Psychrometrics. In M. S. Owen (Ed.), *Handbook of Fundamentals*. Atlanta, Ga.: ASHRAE.

Bhatta, R., Tajima, K., Takusari, N., Higuchi, K., Enishi, O., & Kurihara, M. (2006). Comparison of sulfur hexafluoride tracer technique, rumen simulation technique, and *in vitro* gas

production techniques for methane production from ruminant feeds. *Intl. Congress Series, 1293*, 58-61. http://dx.doi.org/10.1016/j.ics.2006.03.075.

Bhatta, R., Enishi, O., & Kurihara, M. (2007). Measurement of methane production from ruminants. *Asian-Australasian J. Animal Sci., 20*(8), 1305-1318. http://dx.doi.org/10.5713/ajas.2007.1305.

Casey, K. D. (2005). The determination of ammonia emissions from mechanically ventilated poultry houses: An examination of the issues involved. PhD diss. Lexington, Ky.: University of Kentucky, Department of Biosystems and Agricultural Engineering.

Ellis, J. L., Kebreab, E., Odongo, N. E., Beauchemin, K., McGinn, S., Nkrumah, J. D., Moore, S. S., Christopherson, R., Murdock, G. K., McBride, B. W., Okine, E. K., & France, J. (2009). Modeling methane production from beef cattle using linear and nonlinear approaches. *J. Animal Sci., 87*(4), 1334-1345. http://dx.doi.org/10.2527/jas.2007-072.

EPA. (2013). Inventory of U.S. greenhouse gas emissions and sinks: 1990-2011. EPA 430-R-11-005. Washington, D.C.: U.S. Environmental Protection Agency.

Gates, R. S., Casey, K. D., Wheeler, E. F., Xin, H., & Pescatore, A. J. (2008). U.S. broiler housing ammonia emissions inventory. *Atmos. Environ., 42*(14), 3342-3350. http://dx.doi.org/10.1016/j.atmosenv.2007.06.057.

Gates, R. S., Casey, K. D., Xin, H., & Burns, R. T. (2009). Building emissions uncertainty estimates. *Trans. ASABE, 52*(4), 1345-1351. http://dx.doi.org/10.13031/2013.27784.

Grainger, C., Clarke, T., McGinn, S. M., Auldist, M. J., Beauchemin, K. A., Hannah, M. C., Waghorn, G. C., Clark, H., & Eckard, R. J. (2007). Methane emissions from dairy cows measured using the sulfur hexafluoride (SF6) tracer and chamber techniques. *J. Dairy Sci., 90*(6), 2755-2766. http://dx.doi.org/10.3168/jds.2006-697.

Hellwing, A. L. F., Lund, P., Weisbjerg, M. R., Brask, M., & Hvelplund, T. (2012). Technical note: Test of a low-cost and animal-friendly system for measuring methane emissions from dairy cows. *J. Dairy Sci., 95*(10), 6077-6085. http://dx.doi.org/10.3168/jds.2012-5505.

IPCC. (2006). *2006 IPCC Guidelines for National Greenhouse Gas Inventories*. Hayama, Japan: Institute for Global Environmental Strategies.

ISO. (2008). Uncertainty of measurement: Part 3. Guide to the expression of uncertainty in measurement (GUM:1995). ISO/IEC Guide 98-3:2008. Geneva, Switzerland: International Standards Organization.

Johnson, K. A., & Johnson, D. E. (1995). Methane emissions from cattle. *J. Animal Sci., 73*(8), 2483-2492.

Kelly, J. M., Kerrigan, B., Milligan, L. P., & McBride, B. W. (1994). Development of a mobile, open-circuit indirect calorimetry system. *Canadian J. Animal Sci., 74*(1), 65-71. http://dx.doi.org/10.4141/cjas94-010.

Maia, G. D. N., Day, G. B., Gates, R. S., & Taraba, J. L. (2012). Ammonia biofiltration and nitrous oxide generation during the start-up of gas-phase compost biofilters. *Atmos. Environ., 46*(0), 659-664. http://dx.doi.org/10.1016/j.atmosenv.2011.10.019.

Maia, G. D. N., Ramirez, B. C., Green, A. R., Sun, Y., Rodriguez, L. F., Shike, D. W., & Gates, R. S. (2015). A novel ruminant emission measurement system: Part II. Commissioning. *Trans. ASABE* (in review).

Makkar, H. P. S., & Vercoe, P. E., Eds. (2007). *Measuring Methane Production from Ruminants.* Dordrecht, The Netherlands: Springer. http://dx.doi.org/10.1007/978-1-4020-6133-2.

McGinn, S. M. (2006). Measuring greenhouse gas emissions from point sources in agriculture. *Canadian J. Soil Sci., 86*(3), 355-371. http://dx.doi.org/10.4141/S05-099.

McGinn, S. M., Beauchemin, K. A., Coates, T., & Colombatto, D. (2004). Methane emissions from beef cattle: Effects of monensin, sunflower oil, enzymes, yeast, and fumaric acid. *J. Animal Sci., 82*(11), 3346-3356.

McLean, J., & Tobin, G. (1987). *Animal and Human Calorimetry.* Cambridge, U.K.: Cambridge University Press.

Moody, L. B., Li, H., Burns, R. T., Xin, H., Gates, R. S., Hoff, S. J., & Overhults, D. (2008). A quality assurance project plan for monitoring gaseous and particulate matter emissions from broiler housing (sections 1-6). St. Joseph, Mich.: ASABE.

Muñoz, C., Yan, T., Wills, D. A., Murray, S., & Gordon, A. W. (2012). Comparison of the sulfur hexafluoride tracer and respiration chamber techniques for estimating methane emissions and correction for rectum methane output from dairy cows. *J. Dairy Sci., 95*(6), 3139-3148. http://dx.doi.org/10.3168/jds.2011-4298.

Murray, P. J., Moss, A., Lockyer, D. R., & Jarvis, S. C. (1999). A comparison of systems for measuring methane emissions from sheep. *J. Agric. Sci., 133*(4), 439-444. http://dx.doi.org/10.1017/S0021859699007182.

Nienaber, J. A., & Maddy, A. L. (1985). Temperature-controlled multiple chamber indirect calorimeter: Design and operation. *Trans. ASAE, 28*(2), 555-560. http://dx.doi.org/10.13031/2013.32297.

Pinares-Patiño, C. S., & Waghorn, G. C. (Eds.). (2012). *Technical Manual on Respiration Chamber Designs*. Wellington, New Zealand: Ministry of Agriculture and Forestry.

Pinares-Patiño, C. S., Lassey, K. R., Martin, R. J., Molano, G., Fernandez, M., MacLean, S., Sandoval, E., Luo, D., & Clark, H. (2011). Assessment of the sulphur hexafluoride (SF_6) tracer technique using respiration chambers for estimation of methane emissions from sheep. *Animal Feed Sci. Tech., 166-167*, 201-209. http://dx.doi.org/10.1016/j.anifeedsci.2011.04.067.

Place, S. E., Pan, Y., Zhao, Y., & Mitloehner, F. M. (2011). Construction and operation of a ventilated hood system for measuring greenhouse gas and volatile organic compound emissions from cattle. *Animals, 1*(4), 433-446. http://dx.doi.org/10.3390/ani1040433.

Price, J. E., & Lacey, R. E. (2003). Uncertainty associated with the gravimetric sampling of particulate matter. ASAE Paper No. 034116. St. Joseph, Mich.: ASAE.

Ramirez, B. C. (2014). Design and evaluation of open-circuit respiration chambers for beef cattle. MS thesis. Urbana, Ill.: University of Illinois at Urbana-Champaign, Department of Agricultural and Biological Engineering.

Ramirez, B. C., Maia, G. D. N., Green, A. R., Shike, D. W., Rodríguez, L. F., & Gates, R. S. (2013). Design and validation of a calibrated orifice meter for sub-500 liter per minute flow rate applications. ASABE Paper No. 1618475. Joseph, Mich.: ASABE.

Ramirez, B. C., Maia, G. D. N., Green, A. R., Shike, D. W., Rodriguez, L. F., & Gates, R. S. (2014). Design and validation of a precision orifice meter for ventilation rate control in open-circuit respiration chambers. *Trans. ASABE, 57*(6), 1865-1872. http://dx.doi.org/10.13031/trans.57.10754.

Schmidhuber, J., & Tubiello, F. N. (2007). Global food security under climate change. *Proc. Natl. Acad. Sci., 104*(50), 19703-19708. http://dx.doi.org/10.1073/pnas.0701976104.

Skoet, J., & Stamoulis, K. (2006). The state of food insecurity in the world: 2006. Rome, Italy: United Nations FAO.

Storm, I. M., Hellwing, A. L. F., Nielsen, N. I., & Madsen, J. (2012). Methods for measuring and estimating methane emission from ruminants. *Animals, 2*(2), 160-183. http://dx.doi.org/10.3390/ani2020160.

Sun, Y. (2013). Quality assurance project plan for a ruminant emission measurement system. MS thesis. Urbana, Ill.:

University of Illinois at Urbana-Champaign, Department of Agricultural and Biological Engineering.
Suzuki, T., McCrabb, G., Nishida, T., Indramanee, S., & Kurihara, M. (2007). Construction and operation of ventilated hood-type respiration calorimeters for *in vivo* measurement of methane production and energy partition in ruminants. In *Measuring Methane Production from Ruminants* (pp. 125-135). Dordrecht, The Netherlands: Springer.
Taylor, B. N., & Kuyatt, C. E. (1994). Guidelines for evaluating and expressing the uncertainty of NIST measurement results. Gaithersburg, Md.: National Institute for Standards and Technology.
Tomkins, N. W., McGinn, S. M., Turner, D. A., & Charmley, E. (2011). Comparison of open-circuit respiration chambers with a micrometeorological method for determining methane emissions from beef cattle grazing a tropical pasture. *Animal Feed Sci. Tech., 166-167*, 240-247. http://dx.doi.org/10.1016/j.anifeedsci.2011.04.014.